COBEM 2023 27TH INTERNATIONAL CONGRESS OF MECHANICAL ENGENEERING

ABCM Brazilian Society of Mechanical Sciences and Engineering
27th ABCM International Congress of Mechanical Engineering
December 04-08, 2023, Florianópolis-SC, Brazil

COBEM2023-1520 ON THE EVALUATION OF ELATOPLASTIC STRESSES DISTRIBUTION AROUND A CRACK TIP

Mateus B. Neiva
Carlos A. Almeida
Ivan F. M. Menezes
Pontifical Catholic University of Rio de Janeiro (PUC-Rio); Mechanical Engineering Department
mateusbneiva@hotmail.com; calmeida@puc-rio.br; ivan@puc-rio.br

Abstract. *As has been shown by major recent publications, in the evaluation of stresses around a crack tip, throughout numerical simulations, three significant critical difficulties must be overcome: i) the steep high-stress variations in a region close to the tip, ii) the appropriate shape of the crack opening surface and iii) the correctness of the boundary conditions to be accounted for. Although currently available numerical tools can be used to surpass such difficulties as the Finite Element Method (FEM), the first mentioned difficulty may require robust and very refined models, a significant drawback in the convergence process to the numerical solution. In this work, a review of the numerical elastoplastic analysis of a classical problem in fracture mechanics is considered and evaluated and, based on the encountered difficulties, a semi-analytical procedure is then proposed to provide stress and strain distributions around a prescribed crack tip shape. A brief review of the recently published analytical results for solutions under elastic and elastoplastic material behaviors such the Williams and the HRR models, both possessing singular stress distribution fields, and the Creager-Paris modeling with a non-singular stress field, but having the material in the elastic range approach, are considered. Some numerical solutions with these modeling approaches are evaluated with the results obtained using 3D regular finite element discretization using the elastoplastic von Mises yielding criteria employed for the modeling of the crack tip blunt. Next, a semi-analytical model is proposed and discussed in the numerical solution considering the stress function definition as a state variable, with the material in the elastoplastic regime at the blunted crack, considering the crack face as with an elliptical shape. The major advantages of the proposed procedure are discussed in light of its accuracy and robustness.*

Keywords: *Finite Element Method, Fracture Mechanics, Plasticity, Semi-analytical procedure, Elliptical shape crack face*

1. INTRODUCTION

The evaluation of a crack presence is of paramount importance in engineering practice, such as the design and life prediction of mechanical components. These tasks are generally achieved by mechanical behavior evaluations using the numerical simulation of crack effects and their growth. For example, in high cycle fatigue crack growth analysis (FCG), the damage extension and integrity of a component are of study considerations, whereas for material linear elastic behavior stress intensity factor (SIF) is adopted for the prediction of crack propagation.

Although being an important step in fracture mechanics understanding, the SIF as a single-driven force of FCG does not provide all the required answers considering realistic variable amplitude loadings. For instance, it has been observed that material memory effects can delay, arrest or accelerate the FCG rate after an overload has been reached. Moreover, local material plasticity due to cyclic loading ahead of a crack tip is not well described by a single linear elastic parameter without a somehow adjustment, simply because SIF superposition of solutions is not a possible solution. Some additional methods were then elaborated to predict the appropriate changes in FCG rates.

One of the first publications to use a simple phenomenological method to estimate the FCG rate in a cracked model was proposed by Willenborg *et al.* (1971) to treat the overload phenomenon. A similar method was proposed by Wheeler (1972). However, these procedures are too simplistic for not providing accurate mechanical analysis responses.

Elber (1970, 1971) proposed a method to control FCG rate that, instead of using the range of SIF as the driven force, employs the effective stress intensity factor range (ΔK_{eff}), a parameter dependable on the load that opens the crack (P_{op}).

Later, Newman Jr (1981) proposed a FEM formulation for the analysis of 1D structures, using a strip-yield material model to obtain P_{op}, which provides the ΔK_{eff} to perform FCG.

The critical-damage method for FCG prediction that provides modeling and numerical representation with stronger physical arguments was proposed in (Durán *et al.*, 2003), (Castro *et al.*, 2007) and (Castro *et al.*, 2009). It estimates that a volume element "breaks" whenever the accumulated damage reaches its maximum allowed value. In (Ferreira, 2018) a model similar to Newman's strip-yield, applying 1D elements placed along the plastic zone ahead of the crack tip, was used as presented in Fig. 1. In this model, every element is represented as a fatigue ϵN specimen, allowing damage calculations for every load event. A mandatory condition in this model is the use of non-singular stress field condition, otherwise the damage would also present such singular distribution.

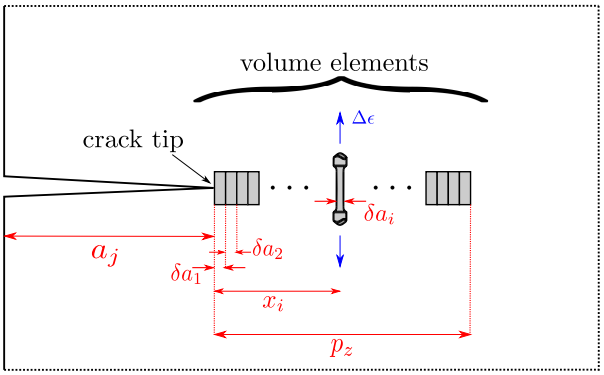

Figure 1: Critical-damage for FCG problem prediction (Durán *et al.*, 2003)

2. CLASSICAL FRACTURE MECHANICS PROBLEM

In this section, the simulation of a cracked specimen employing the finite element modeling is considered. Details of the implemented model to achieve better and realistic stress and strain fields occurring at the region ahead of the crack tip are also discussed by Neiva (2021).

Regarding the material constitutive behavior in Fracture Mechanics, concerning published analytical solutions, two approaches are employed: the Linear Elastic Fracture Mechanics (LEFM) with theoretical solutions offered in (Williams, 1957) and (Creager and Paris, 1967) and the Elastoplastic Fracture Mechanics (EPFM) HRR solutions, in (Hutchinson, 1968).

The finite element model used: a) no enrichment in the element's interpolation function subspace, no procedure used to represent a possible stress singularity occurrence at the crack tip where plasticity occurs due to blunting, as loading increases; and b) material models including plasticity effects to obtain a realistic specimen's mechanical behavior, of the material peculiarities close to the crack tip.

Due to the occurrence of high stress component values (stress concentration) at a small region of the cracked specimen, the material ought to have a plastic behavior characterizing a plastic zone. The high stress gradient occuring in this region required, in the analysis discretization, the use of second-order 10-node tetrahedron elements ($T10$).

The specimen geometry considered is shown in Fig. 2. Due to symmetry, only one-fourth is represented in the numerical model, consisting of a tensioned central cracked plate under a self-equilibrated distributed loading, applied in a direction normal to the crack. In this case, the SIF in mode I (K_I) and the J-integral (J) are, thus, well-known parameters as presented in (Castro and Meggiolaro, 2016).

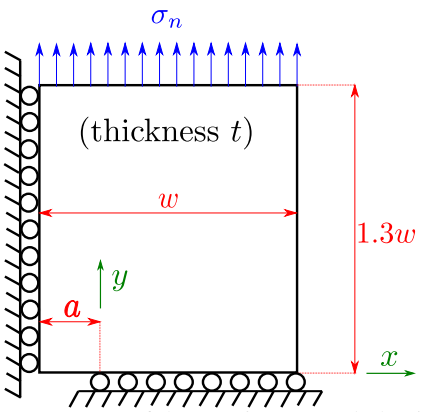

Parameters	Num. Values	Units
σ_n	$180 \cdot 10^6$	Pa
a	0.025	m
w	0.1	m
t	0.01	m

Figure 2: Geometry (1/4 of the speciment) and physical parameters considered in the numerical model analysis.

The material hardening law employed is described by dimensionless Ramberg-Osgood model (1943), the same used in HRR model derivations, as $\sigma_y = 300\ MPa$, $E = 210\ GPa$, $\alpha = 0.02\ GPa$ and $n = 13$.

The result presentation comprises the main objectives for evaluating distribution of σ_{yy} along the specimen residual ligament by comparing it to other proposed methods.

The presentation of the analysis results at points ahead of the crack, located at distances from the tip in multiples of the plastic zone length, are then considered. These point locations are presented in Fig. 3, showing in distinct color shades the material occurence in two regimens, plastic or elastic. The mid-section plastic zone length is used here as the reference length of the plastic zone. Thus, in this regard, as shown in Fig. 3, a point at $0.8\%p_z$ on the upper surface is, in fact, under

the elastic regime, due to the parabolic-like shape of the plastic zone throughout the specimen thickness.

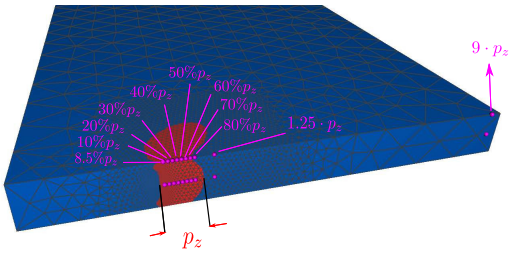

Figure 3: Plastic zone characterization. In blue elastic and in red is plastic.

2.1 RESIDUAL LIGAMENT EVALUATION

The numerical values of stresses and strains obtained along the specimen residual ligament region at full ligament, at the plastic zone, and, finally, close to the crack tip, are considered in this section. Over the length of full ligament, where the material is in the elastic regime, length p_z is equal to $8.06 \cdot 10^{-3}\ m$ and the specimen bound is roughly $9 \cdot p_z$, as shown in Fig. 3. Besides, the elastoplastic HRR stress field and the William and Creager-Paris linear elastic stress solutions are also presented, for comparison.

Concerning the Creager-Paris analytical model, the curvature of the blunted crack was obtained from the finite element analysis results considering y-direction displacements along the length of the crack stress-free face, as illustrated in Fig. 4.

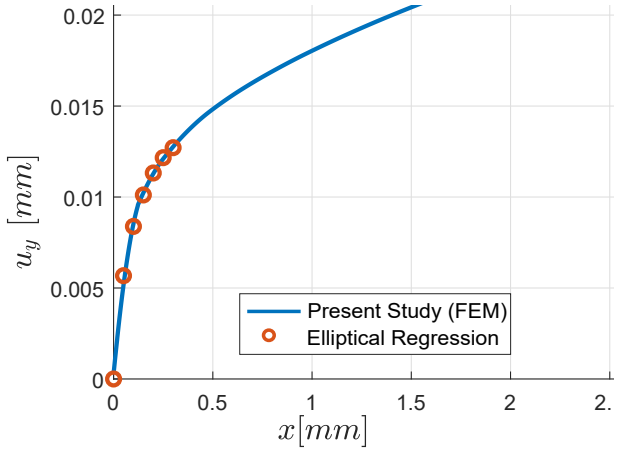

Figure 4: Path plot of u_y as a function of the residual ligament.

For the results close to the crack tip a data regression was performed. A nonlinear least-squares solver optimization algorithm was used to reduce error differences from FEM data and the equation of an ellipse, which resulted in the following geometric parameters

a	$3.7401 \cdot 10^{-4}\ m$
b	$1.3070 \cdot 10^{-5}\ m$
c	$3.7378 \cdot 10^{-4}\ m$
ρ	$4.5675 \cdot 10^{-7}\ m$

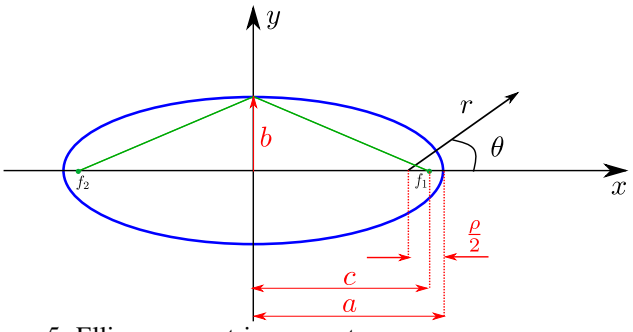

Figure 5: Ellipse geometric parameters.

Also, in plane-stress conditions, a comparison of numerically obtained stress σ_{yy} results with the solutions provided by Williams, Creager-Paris, and HRR models are presented in Fig. 6. It may be observed that the three above mentioned

analytical solutions do not guarantee the required equilibrium condition at the position $9 \cdot p_z$ in the residual ligament as indicated in dashed line. However, this condition is adequately satisfied by the FEM numerical solutions, with its validation by considering the Saint-Venant's principle.

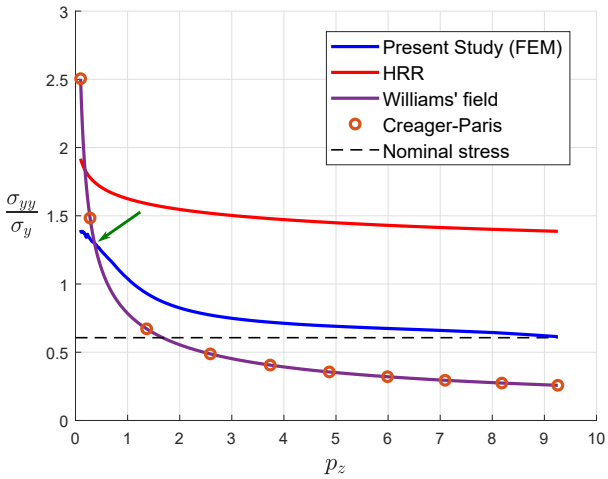

Figure 6: Path plot for σ_{yy}/σ_y along the residual ligament (at plate mid-section).

Equilibrium is no longer guaranteed by the analytical solutions, once they are only valid at a region close to the crack tip. From Fig. 6, it can also be inferred that the Williams solution meets the numerical (FEM) solution at a location close to $0.36p_z$. In the case of the HRR field, which uses the elasticity formulation, the solution along the residual ligament is quite apart from the expected numerical analysis, predicting a plastic collapse over the cross-section.

Although the Creager-Paris model provides a non-singular analytical solution, because of the assumed curvature at the crack tip, no significant differences to Williams' solution are observed, reinforcing the need to consider in the model the material elastoplastic behavior. Focusing on results in Fig. 6, where the plastic zone in FEM and HRR solutions are relevant (i.e., $x \leqslant 1.0 \cdot p_z$), Fig. 7 shows significant result discrepancies in this region, even though elastic contributions have been neglected in the analytical solution available.

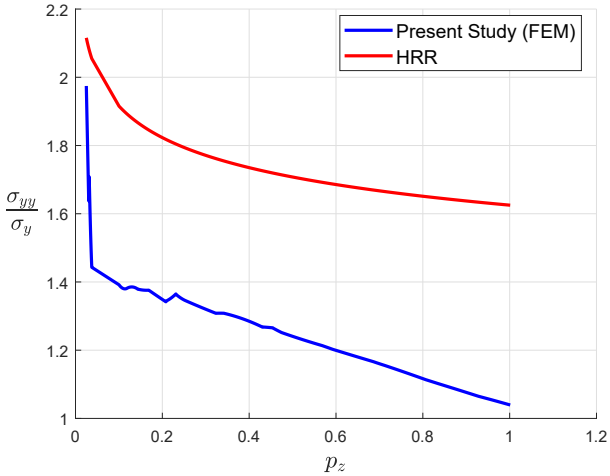

Figure 7: Path plot of σ_{yy} as function of the residual ligament (at plate mid-section).

In considering the numerical results at a region very close to the crack tip, solutions in (McMeeking and Parks, 1979) present numerical results using 2D elastoplastic FEM with small and large scale yielding for both stress and strain plane conditions. As a reference, the geometric and material parameters in this simulation were somehow adapted for the respective values considered by the authors. For this case only, geometric and material parameters used in the model are given in Table 1.

Table 1: Geometric, material and load parameters

Parameters	**Num. Values**	**Units**
σ_n	$180 \cdot 10^6$	Pa
E	$120 \cdot 10^9$	Pa
σ_y	$400 \cdot 10^6$	Pa
α	$0.02 \cdot 10^9$	Pa
n	10	$-$
a	0.05	m
w	0.1	m
t	0.01	m

A comparison of normalized stresses to normalized positions, along the residual ligament for three model solutions: HRR, FEM, and (McMeeking and Parks, 1979) are shown in Fig. 8. FEM elastoplastic solutions are obtained using 3D simulation. Straining restrictions assumed in direction transverse to the specimen plane resulted in higher plasticity conditions, which are not capable to provide stresses as low as in large strains approach as presented in (McMeeking and Parks, 1979). Moreover, both numerical results present peak values at the same $x-$coordinate position.

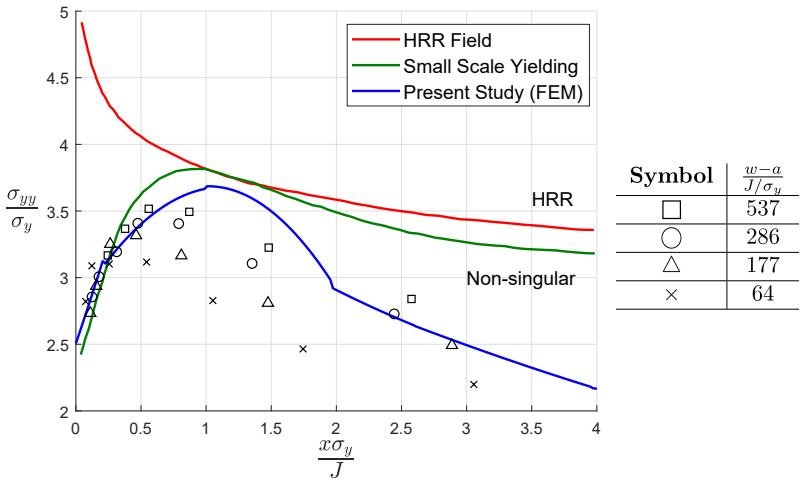

Figure 8: Normalized stresses on a plane ahead of crack tip for $\sigma_y/E = 1/300$ and $a/w = 0.5$ (at plate mid-section).

The obtained numerical results are compatible with the dispersed numerical data and predict a large error when comparing to HRR at the bottom right of Fig. 8, which was previously noticed also in Fig. 7.

3. NHRR METHODOLOGY

In order to establish the stress and strain fields, a similar strategy as in HRR model is proposed, which consists in obtaining a stress function field that verifies the strain compatibility equation and boundary conditions for a singular crack condition using polar coordinates. Thus, as considered in the (Creager and Paris, 1967) model, a proposed NHRR model uses an elliptical crack face shape, with the elliptical coordinates to impose the appropriate boundary conditions. In this regard, to establish the NHRR model, Airy's functions and strain compatibility equations are required, all expressed in elliptical coordinates (ξ, η), as shown in Fig. 9.

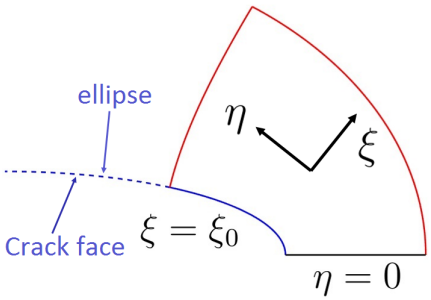

Figure 9: Cartesian domain

We start from the following definition, in a cartesian coordinate system for stresses definition:

$$\begin{cases} \sigma_{xx} = \frac{\partial^2 \Psi}{\partial y^2} \\ \sigma_{yy} = \frac{\partial^2 \Psi}{\partial x^2} \\ \sigma_{xy} = -\frac{\partial^2 \Psi}{\partial x \partial y} \end{cases} \tag{1}$$

and, for the compatibility conditions

$$C = \frac{\partial^2 \epsilon_{xx}}{\partial y^2} - 2 \cdot \frac{\partial^2 \epsilon_{xy}}{\partial x \partial y} + \frac{\partial^2 \epsilon_{yy}}{\partial x^2} = 0 \tag{2}$$

A tensor transformation must then be employed for a rotation angle θ. In opposite to the polar system where θ is an independent coordinate (as illustrated in Fig. 11), in elliptical coordinates the angle θ is dependent on both coordinates (ξ, η), as in Fig. 10. As an immediate result, the strain compatibility equations (PDEs) can not be solved using the usual separation of variables technique, as adopted in the original HRR model, and reducing them to ODEs. In practice, in the NHRR model, the resulting system of equations must be solved as PDEs in a bi-dimensional domain.

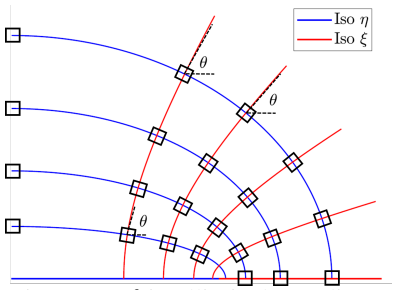

Figure 10: θ in elliptical coordinate

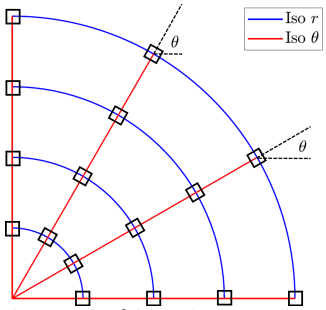

Figure 11: θ in polar coordinate

As in continuum mechanics, three equations must be applied to solve a structural elastoplastic problem. Besides Airy's function definitions and the compatibility equation, strain tensor components definition should be established, requiring a hardening law similar to the HRR model, taking advantage of the elliptical orthonormal coordinate systems. This results in

$$\epsilon_{ij} = \frac{3}{2} \frac{\alpha}{E} \left(\frac{\sigma_e}{\sigma_y} \right)^{n-1} \cdot S_{ij} \tag{3}$$

where α and n are hardening parameters from Ramberg and Osgood (1943) material law, σ_e is the von Mises equivalent stress, E is the Young's modulus, σ_y is yield stress and S_{ij} is the deviatoric $i - j$ stress component.

For considering the transversal stress component, Guo (1993) suggests the Tz-function as

$$T_z = \frac{\sigma_{33}}{\sigma_{11} + \sigma_{22}} \tag{4}$$

T_z is bounded in $[0, 0.5]$ interval, presenting two limit cases: plane-stresses, for $T_z = 0$, and $T_z = 0.5$ for plane-strains. Notice that σ_e and S_{ij} are both dependent on a given T_z.

In the $2D$ cartesian domain with elliptical coordinates, illustrated in Fig. 9, the initial coordinate ξ_0 defines the crack face. At the same time, $\eta = 0$ represents a symmetry plane, where only half of the domain is considered. A resulting 4th-order PDE requires four boundary conditions, as follows: (a) in the crack face, where no traction vector occurs, free wall condition: the normal stress $(\sigma_{\xi\xi})$ and shear stress $(\sigma_{\xi\eta})$ are set to zero and (b) in the residual ligament, with elliptical coordinate $\eta = 0$, symmetry condition should be imposed, with the shear stress $(\sigma_{\xi\eta})$ and the derivatives of the tangential and normal stresses $(\sigma_{\xi\xi}, \sigma_{\eta\eta})$, with respect to the normal coordinate η, all being set to zero. These conditions result in the following

$$\begin{cases} \sigma_{\xi\xi} = 0 \text{ and} \\ \sigma_{\xi\eta} = 0, \text{at } \xi = \xi_0 \\ \sigma_{\xi\eta} = 0 \text{ and} \\ \frac{\partial \sigma_{\xi\xi}}{\partial \eta} = 0 \text{ and} \\ \frac{\partial \sigma_{\eta\eta}}{\partial \eta} = 0, \text{at } \eta = 0 \end{cases} \tag{5}$$

Without loss of generality, instead of obtaining the total stress function state variable (Ψ), a parametric stress function $(\tilde{\Psi})$ is considered, expliciting an amplitude K-factor, which allows to adjust the total stress function to a giving load or boundary condition, in the form

$$\Psi = K \cdot \tilde{\Psi} \tag{6}$$

Since no unique solution for the total stress function (Ψ) that validates boundary conditions has been obtained, a convenient parameter, derived for elastoplastic fracture mechanics, to restrict the sought solution is used: the J-integral. In this way, the K-factor amplitude is obtained with the J-integral performed over the domain's boundaries, depicted in Fig. 9. Using the J-integral, a path-independent parameter is quite convenient, allowing changes in the domain size and computing stress and strain fields close to the crack tip without additional boundary and load conditions. As defined by Rice (1968) in cartesian coordinates, it is given by

$$J(\Psi) = \oint_S \left[U \, dy - T_i \frac{\partial u_i}{\partial x} \, ds \right] \tag{7}$$

and for a given value of J an amplitude of K-factor is obtained, which recovers the total stress function defined in the analysis domain, and, consequently, the stress and strain distribution fields.

4. CONCLUSIONS

From considering the evaluation of a classic crack opening using semi-analytic stress solutions compared to numerical FEM results, a model to the problem is proposed, the NHRR, which solution verifies the three major continuum mechanics requirements: equilibrium, correct boundary conditions, and elastoplastic material behavior.

An important characteristic of this proposed model is its paramount difference as compared to standard FEM. If the virtual work theorem is applied with displacements as state variables in the later problem, the total stress function is the sole variable in the semi-analytic solution. Also, when it comes to apply the virtual work principle, displacements and loads are explicitly stated, providing a clear physical interpretation of the variables involved. Although this fact is certainly an advantage in using the FEM, it requires an explicit domain definition where displacements and/or loads are prescribed, resulting in large-scale models, specially considering crack problems. On the other hand, by imposing the compatibility condition as in the NHRR, stress distributions are established in the geometric domain. Even though it still requires equilibrium conditions to be imposed, it is mechanically equivalent to the energy balance approach, and the sough solution focuses on mathematical derivations explicitly. As a result, a powerful tool for locally computing the stress and strain fields is obtained.

5. ACKNOWLEDGEMENTS

The authors acknowledge the financial support provided by CNPq and "Coordenação de Aperfeiçoamento de Pessoal de Nível Superior - Brasil" (CAPES).

6. REFERENCES

Castro, J. and Meggiolaro, M., 2016. *Fatigue Design Techniques Under Real Service Loads - Volume III - Crack Propagation, Temperature and Statistical Effects*.

Castro, J., Meggiolaro, M. and Miranda, A., 2007. "A note on fatigue crack growth predictions based on damage accumulation ahead of the crack tip." *Solid Mechanics in Brazil*, pp. 133–146.

Castro, J., Meggiolaro, M. and Miranda, A., 2009. "Fatigue crack growth predictions based on damage accumulation calculations ahead of the crack tip." *Comput Mat Sci*, Vol. 46, pp. 115–123.

Creager, M. and Paris, P., 1967. "Elastic field equations for blunt cracks with reference to stress corrosion cracking". *Int J Fract Mech*, Vol. 3, pp. 247–252.

Durán, J., Castro, J. and Payão Filho, J., 2003. "Fatigue crack propagation prediction by plasticity damage accumulation models." *Fatigue Fract Eng Mater Struct*, Vol. 26, pp. 137–150.

Elber, W., 1970. "Fatigue crack closure under cyclic tension." *Eng Fract Mech*, Vol. 2, pp. 37–45.

Elber, W., 1971. "The significance of fatigue crack closure." *ASTM STP*, Vol. 486, pp. 230–242.

Ferreira, S.E., 2018. *Modelagem da Propagação da Trinca de Fadiga Através do Dano Acumulado na Zona Plástica*. Ph.D. thesis, Graduate Program in Mechanical Engineering, Pontifícia Universidade Católica do Rio de Janeiro, Rio de Janeiro, Brasil.

Guo, W., 1993. "Elastoplastic three dimensional crack border field - I. singular structure of the field". *Engineering Fracture Mechanics*, Vol. 46, pp. 93–104.

Hutchinson, J., 1968. "Singular behaviour at the end of a tensile crack tip in a hardening material". *J Mech Phys Solids*, Vol. 16, pp. 13–31.

McMeeking, R. and Parks, 1979. "A criterion for j-dominance of crack-tip fields in a large scale yielding". *ASTM STP*, Vol. 668, pp. 175–194.

Neiva, M.B., 2021. *3D Numerical Elastoplastic Analysis of Stress and Strain Distribution Around Crack Tips*. Master's thesis, Graduate Program in Mechanical Engineering, Pontifícia Universidade Católica do Rio de Janeiro, Rio de Janeiro, Brasil.

Newman Jr, J., 1981. "A crack-closure model for predicting fatigue crack growth under aircraft spectrum loading." *ASTM STP*, Vol. 748, pp. 53–84.

Ramberg, W. and Osgood, W.R., 1943. "Description of stress–strain curves by three parameters". *National Advisory Committee For Aeronautics*, Vol. Technical Note No. 902.

Rice, J.R., 1968. "A path independent integral and the approximate analysis of strain concentration by notches and cracks". *J App Mech*, Vol. 35, pp. 379–386.

Wheeler, O., 1972. "Spectrum loading and crack growth." *J Basic Eng*, Vol. 94, pp. 181–186.

Willenborg, J., Engle, R. and Wood, H., 1971. "Crack growth retardation model using an effective stress concept". *Wright Patterson Air Force Laboratory*.

Williams, M., 1957. "On the stress distribution at the base of a stationary crack". *J App Mech*, Vol. 24, pp. 109–114.

7. RESPONSIBILITY NOTICE

Mateus B. Neiva, Carlos A. Almeida and Ivan F. M. Menezes are solely responsible for the printed material included in this paper.